29th EPS Conference on Plasma Phys. and Contr. Fusion Montreux, 17-21 June 2002 ECA Vol. **26B**, P-4.102 (2002)

Comparisons between Semi-Lagrangian Drift-Kinetic Code and PIC Code Simulations for ITG Studies

M. Brunetti, V. Grandgirard[1], S. Allfrey, A. Bottino, P. Bertrand[2], P. Ghendrih[1], O. Sauter, J. Vaclavik, L. Villard

CRPP, Association Euratom-Confédération Suisse, EPFL, 1015 Lausanne, Switzerland

[1]*DRFC, Association Euratom-CEA, CEA Cadarache, 13108 St Paul-lez-Durance, France*

[2]*LPMIA, Université Henri Poincaré-Nancy 1, BP 239, 54506 Vandoeuvre-les-Nancy, France*

1 Introduction

In this paper we focus on micro-instabilities destabilized by spatial inhomogeneities, particularly those driven by ion temperature gradients (ITG), which are commonly considered leading candidates to explain the anomalous transport in magnetically confined fusion plasmas. Nonlinear gyrokinetic simulations play an important role in understanding the physics of these micro-instabilities [1]. We present results obtained with a recently developed semi-Lagrangian (SL) code both in the linear and the non-linear regime of the ITG instability, and we compare these results with those obtained with Particle in Cell (PIC) codes which solve the same equations [2, 3].

2 Semi-Lagrangian code

In the SL code, a uniform magnetic field $\vec{B} = B\hat{z}$ in a periodic cylindrical plasma is considered, electrons are assumed adiabatic and finite Larmor radius effects are neglected. Thus, the characteristics of the ions are the guiding-centre (GC) trajectories

$$\vec{v}_{GC} = \frac{\vec{E}\times\vec{B}}{B^2}, \qquad \frac{dz}{dt} = v_{||}, \qquad \dot{v}_{||} = \frac{q}{m_i}E_z \tag{1}$$

$\vec{E}$ being the electric field, $q = Ze$ and m_i the ion charge and mass, respectively. The ion distribution function $f(r,\theta,z,v_{||},t)$ obeys

$$\frac{\partial f}{\partial t} + \vec{v}_{GC}\cdot\vec{\nabla}_\perp f + v_{||}\frac{\partial f}{\partial z} + \dot{v}_{||}\frac{\partial f}{\partial v_{||}} = 0 \tag{2}$$

The system of equations is closed by invoking quasi-neutrality

$$-\vec{\nabla}_\perp\cdot\left[\frac{n_0(r)}{B\Omega_{ci}}\vec{\nabla}_\perp\Phi\right] + \frac{en_0(r)}{T_e(r)}(\Phi - <\Phi>) = n_i - n_0 \tag{3}$$

where the first term on the left hand side is the polarization term, $\Phi(r,\theta,z,t)$ is the electric potential, $\vec{E} = -\vec{\nabla}\Phi$, $< . >$ represents the average on the magnetic field lines,

$n_i(r,\theta,z,t)$ is the ion density, $n_0(r)$ is the equilibrium density, $T_e(r)$ is the electron temperature profile and $\Omega_{ci} = qB/m_i$. The integration of the Vlasov equation, Eq. (2), is performed using a time-splitting method and the fact that f is constant along the characteristics of the particles [4, 5]. The Poisson equation, Eq. (3), is solved using a finite element method. The plasma is initialized by exciting a superposition of ITG modes (m,n) with random phases and amplitudes, $f(r,\theta,z,v_{\|},0) = f_M[1+h(v)g(r)\sum_{mn}\epsilon_{mn}\cos(2\pi nz/L_z + m\theta + \alpha_{mn})]$, where $f_M(r,v_{\|}) = \left(n_0/\sqrt{2\pi T_i/m_i}\right)\exp(-m_i v_{\|}^2/2T_i)$, L_z is the cylinder length, and h and g are fourth order polynomials with Dirichlet boundary conditions. The results presented here correspond to simulations with a $(128\times 64\times 32\times 64)$ discretization and $dt = 1$.

3 Linear regime

In order to compare the results of the SL code with analytical values, we neglect the polarization term in Eq. (3) and we consider a flat density profile, $n_0 =$ constant. Moreover, we set the cylinder length to $L_z/\rho_s = 628$ (where $\rho_s = \sqrt{k_B T_{e0}\, m_i}/eB$), the radius to $L_r/\rho_s = 10$ and the electron temperature profile to a constant. The ion temperature profile is such that $d\ln T_i/dr = -\kappa_T \cosh^{-2}[(r-r^*)/\Delta r_T]$ (with $\kappa_T = 4$, $\Delta r_T/\rho_s = 0.1$ and $r^* = 0.5\ L_r$) and $T_i(r^*) = T_{i0} = T_{e0}$. In the limit in which the ITG frequency ω is such that $\omega_{Ti} \gg \omega \gg k_z v_{thi0}$ (where $\omega_{Ti} = (k_\theta/qB)\ dT_i/dr$ is the diamagnetic drift frequency related to the ion temperature gradient and $v_{thi0} = \sqrt{k_B T_{i0}/m_i}$), an unstable mode exists whose growth rate can be analytically estimated and is given by $\gamma = \sqrt{3}\ |k_z^2\ v_{thi0}^2\ \omega_{Ti}|^{1/3}/2$. In Fig. 1 (left), the computed and the analytical values of the growth rate are shown for ITG modes with $n = 4$, $m = 10, ..., 20$. A very good agreement

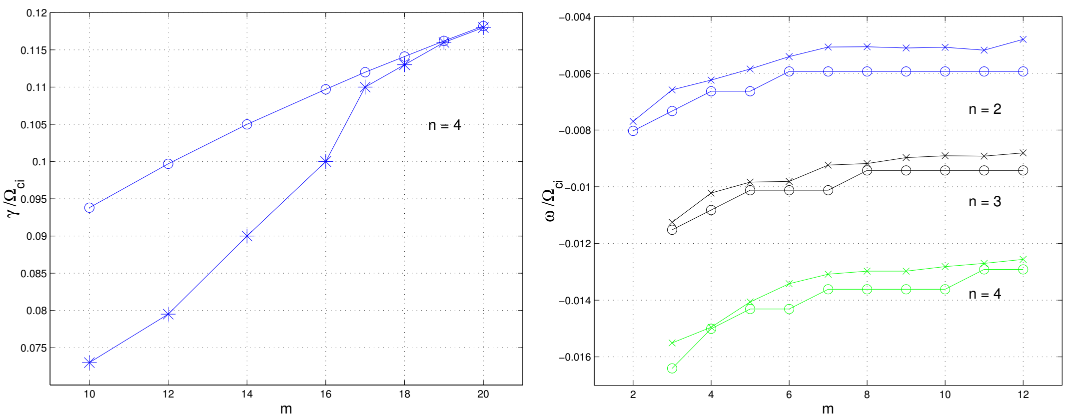

Figure 1: (left) ITG growth rates: numerical ($*$) and analytical (o) values; (right) ITG frequencies: values obtained with the SL code ($\times$) and with LORB5 (o).

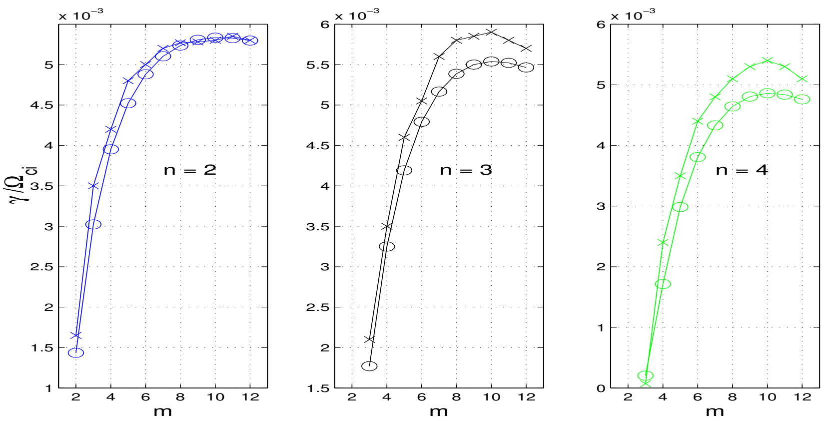

Figure 2: ITG growth rates: values obtained with the SL code (×) and with LORB5 (o).

is reached when the corresponding ITG frequency satisfies the condition in which the analytical formula holds, $\omega \gg k_z v_{thi0} = 0.04\ \Omega_{ci}$ (in the present case for $m > 16$).

When the polarization term is included in Eq. (3), the ITG frequencies and growth rates obtained with the SL code are compared with those obtained with the code LORB5. For the comparisons with the PIC codes we use the following configuration: $L_r/\rho_s = 14.5$, $L_z/\rho_s = 1508$, $\kappa_n = 0.8$, $\Delta r_n/\rho_s = 0.2$, and the other parameters set as before. The electric potential Φ is Fourier filtered in the periodic coordinates, as is done in the PIC codes (the filter retains modes up to $|m| = 16$ and $|n| = 8$). The results are plotted in Fig. 1 (right) and Fig. 2, and show a good agreement between the codes.

4 Non-linear regime

In the non-linear regime, the saturation of the ITG instability occurs. We compare the results obtained with the PIC code ORB5 using 33 million tracers (PIC 33) and 67 million tracers (PIC 67) with those obtained with the SL code. In performing this

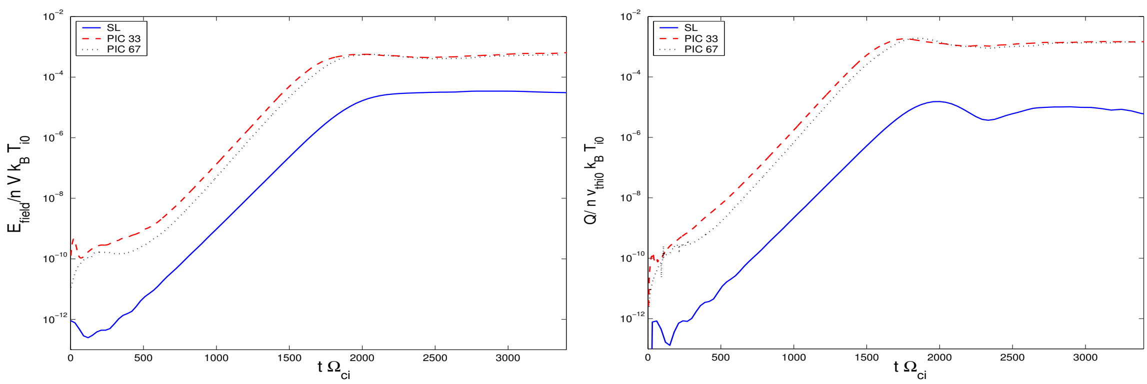

Figure 3: Comparison between the SL code (solid blue), ORB5 with 33 million tracers (dashed red) and ORB5 with 67 million tracers (dotted black): (left) time evolution of the field energy and (right) of the heat flux.

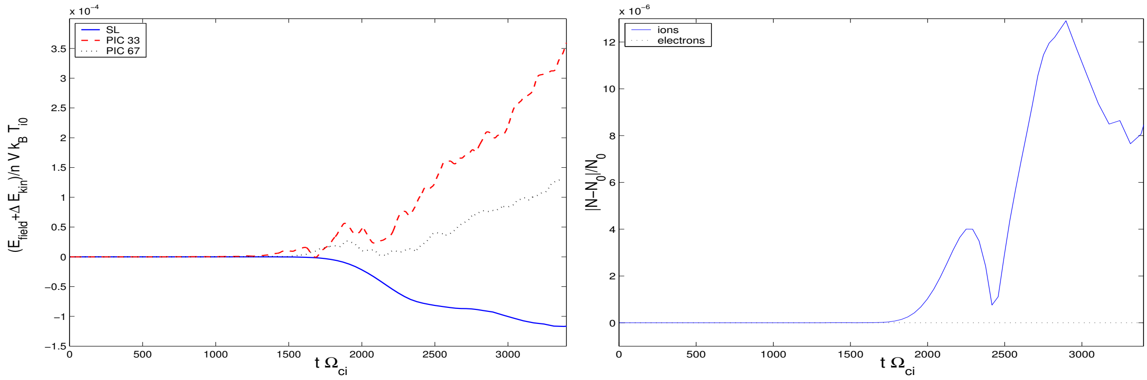

Figure 4: (left) Comparison between the SL code (solid blue), ORB5 with 33 million tracers (dashed red) and ORB5 with 67 million tracers (dotted black): time evolution of the total energy; (right) SL code: time evolution of the relative error in the number of particles.

comparison, we do not include modes with $n = 0$. In Fig. 3 we show the time evolution of the field energy (left) and of the heat flux (right). Even if the overall behavior of these quantities obtained with the two codes is very similar, the level of saturation attained is different (i.e., a factor 100 in the flux). This is an issue that we plan to investigate better in the future. The conservation of the total energy (see Fig. 4, left), which is an important property to verify the quality of a numerical simulation, is equally good in PIC 67 and SL. The latter conserves the number of particles N with a good accuracy (see Fig. 4, right), the relative error in N being of the order of 10^{-5} at the end of the simulation.

5 Conclusions and further work

A SL code has been developed which is able to describe the non-linear phase of the ITG modes instability conserving the total energy of the system to a good accuracy comparable to that attained with the PIC code ORB5. Further investigations are necessary to understand the different level of saturation observed in the heat flux with the two codes.

References

[1] F. Jenko and W. Dorland, *Plasma Phys. Control. Fusion* **43**, A141 (2001) .

[2] A. Bottino et al., *Th. Fusion plasmas* (Proc. Int. Workshop, Varenna, 2000), Ed. Compositori, Bologna, 2001.

[3] T.M. Tran et al., *Th. Fusion Plasmas* (Proc. Int. Workshop, Varenna, 1998), Ed. Compositori, Bologna, 1999.

[4] C.Z. Chen and G. Knorr, *Journal of Comput. Phys.* **22**, 330 (1976) .

[5] E. Sonnendrücker et al., *Journal of Comput. Phys.* **149**, 201 (1999).